

Optimal Runge–Kutta Stability Regions

David I. Ketcheson* Aron J. Ahmadi†

January 14, 2020

Abstract

The stable step size for numerical integration of an initial value problem depends on the stability region of the integrator and the spectrum of the problem it is applied to. We present a fast, accurate, and robust algorithm, based on convex optimization, to select an optimal linearly stable Runge–Kutta stability polynomial of any order and any number of stages, for any initial value problem in which the spectrum of the Jacobian is available. Optimized methods with increased number of stages can be used to enhance the efficiency of many method-of-lines PDE discretizations. Examples of optimal stability polynomials for a variety of problems are given.

1 Stability of Runge–Kutta methods

Runge–Kutta methods are one of the most widely used types of numerical integrators for solving initial value ordinary and partial differential equations. The time step size should be taken as large as possible since the cost of solving an initial value problem (IVP) up to a fixed final time is proportional to the number of steps that must be taken. In practical computation, the time step is often limited by stability and accuracy constraints. Either accuracy, stability, or both may be limiting factors for a given problem; see e.g. [25, Section 7.5] for a discussion. The linear stability and accuracy of an explicit Runge–Kutta method are characterized completely by the so-called stability polynomial of the method, which in turn dictates the acceptable step size [7, 15].

*King Abdullah University of Science and Technology (KAUST), Division of Mathematical and Computer Sciences and Engineering, Thuwal, 23955-6900. Saudi Arabia (david.ketcheson@kaust.edu.sa)

†King Abdullah University of Science and Technology (KAUST), Division of Mathematical and Computer Sciences and Engineering, Thuwal, 23955-6900. Saudi Arabia

In this work we present an approach for constructing a stability polynomial that allows the largest absolutely stable step size for a given problem. The approach described here can speed up the integration of any IVP for which

- explicit Runge–Kutta methods are appropriate;
- the spectrum of the problem is known or can be approximated; and
- stability is the limiting factor in choosing the step size.

Although for simplicity we consider only linear initial value problems, we expect our approach to be useful in designing integrators for nonlinear problems via the usual approach of considering the spectrum of the Jacobian.

The amount of speedup depends strongly on the spectrum of the problem, and can range from a few percent to several times or more. Based on past work and on results presented in Section 3, we expect that the most substantial gains in efficiency will be realized for systems whose spectra have large negative real parts, such as for semi-discretization of PDEs with significant diffusive or moderately stiff reaction components. As demonstrated in Section 3, worthwhile improvements may also be attained for general systems, and especially for systems whose spectrum contains gaps. High order methods will also see greater gains in efficiency, since our results indicate that their efficiency approaches that of low order methods when enough stages are used.

In the remainder of this section, we review the stability concepts for Runge–Kutta methods and formulate the stability optimization problem. Our optimization approach, described in 2, is based on reformulating the stability optimization problem in terms of a sequence of convex subproblems and using bisection. As discussed in Section 2.1, a rigorous theoretical justification for the use of bisection in this way is still lacking. Nevertheless, our scheme consistently finds globally optimal solutions. The question of why bisection seems to always lead to globally optimal solutions merits further investigation.

Another key element of our optimization algorithm, discussed in Section 2.2, is the choice of a polynomial basis that is well-conditioned when sampled over a particular region of the complex plane. This becomes particularly important when the number of stages of the method is allowed to be very large. We do not present a general technique for choosing such a basis, but we do achieve good results for many spectra by some straightforward choices of basis. Better choices of solution basis could make our approach even more robust and accurate.

Determination of the stability polynomial is only half of the puzzle of designing optimal explicit Runge–Kutta methods. The other half is the determination of the Butcher coefficients. While simply finding methods with a desired stability polynomial is straightforward, many additional challenges arise in that context; for instance, additional nonlinear order

conditions, internal stability, storage, and embedded error estimators. The development of full Runge–Kutta methods based on optimal stability polynomials is the subject of ongoing work [30].

The work presented here suggests several extensions. While we have focused primarily on design of the stability properties of a scheme, the same approach can be used to optimize for accuracy efficiency, which is a focus of future work. Our algorithm can also be applied in other ways; for instance, it could be used to impose a specific desired amount of dissipation, for use in multigrid or as a kind of filtering.

One of the most remarkable aspects of our algorithm is its speed, which opens up the potential for a new kind of adaptive time stepping in which the time integration method itself is designed on-the-fly during the computation. For nonlinear problems, the method could be adapted, for instance, when a significant change in the spectrum of the linearized semi-discretization is detected. Whereas traditional automatic integrators dynamically adjust the step size and scheme order, choosing from a small set of pre-selected methods, our algorithm could be used as the basis for an implementation that also automatically adjusts details of the stability polynomial at each step.

We remark that the problem of determining optimal polynomials subject to convex constraints is very general. Convex optimization techniques have already been exploited to solve similar problems in filter design [8], and will likely find further applications in numerical analysis.

1.1 The stability polynomial

A linear, constant-coefficient initial value problem takes the form

$$u'(t) = Lu \qquad u(0) = u_0, \tag{1}$$

where $u(t) : \mathbb{R} \rightarrow \mathbb{R}^N$ and $L \in \mathbb{R}^{N \times N}$. A common numerical solver for (1) is the four-stage fourth-order Runge–Kutta method, which takes the form

$$y_1 = u_n \tag{2a}$$

$$y_2 = u_n + \frac{h}{2}Ly_1 \tag{2b}$$

$$y_3 = u_n + \frac{h}{2}Ly_2 \tag{2c}$$

$$y_4 = u_n + hLy_3 \tag{2d}$$

$$u_{n+1} = u_n + \frac{h}{6} (Ly_1 + 2Ly_2 + 2Ly_3 + Ly_4), \tag{2e}$$

where h is the step size and u_n is a numerical approximation to $u(nh)$. By direct substitution, this simplifies to

$$u_{n+1} = \left(I + hL + \frac{h^2}{2}L^2 + \frac{h^3}{6}L^3 + \frac{h^4}{24}L^4 \right) u_n. \quad (3)$$

In fact, when applied to the linear IVP (1), any Runge–Kutta method reduces to an iteration of the form

$$u_n = R(hL)u_{n-1}, \quad (4)$$

where the *stability function* $R(z)$ depends only on the coefficients of the Runge–Kutta method [12, Section 4.3][7, 15]. In the case of the fourth-order method (2), we see from (3) that $R(z)$ is just the degree-four Taylor approximation of the exponential:

$$R(z) = 1 + z + \frac{z^2}{2!} + \frac{z^3}{3!} + \frac{z^4}{4!}. \quad (5)$$

In general, the stability function of an s -stage, order p , explicit Runge-Kutta method is a polynomial of degree s

$$R(z) = \sum_{j=0}^s a_j z^j. \quad (6)$$

Since the exact solution of (1) is $u(t) = \exp(tL)u_0$, then if the method is accurate to order p , the stability polynomial must be identical to the exponential function up to terms of at least order p :

$$a_j = \frac{1}{j!} \quad \text{for} \quad 0 \leq j \leq p. \quad (7)$$

1.2 Absolute stability

The stability polynomial governs the local propagation of errors, since any perturbation to the solution will be multiplied by $R(z)$ at each subsequent step. The asymptotic growth of errors thus depends on $\|R(hL)\|$, which leads us to define the *absolute stability region*

$$S = \{z \in \mathbb{C} : |R(z)| \leq 1\}. \quad (8)$$

For example, the stability region of the fourth-order method (2) is shown in Figure 1(b).

Given an initial value problem (1), let the set $\sigma(L) = \{\lambda_i\}$ ($i = 1, \dots, N$) denote the eigenvalues of the matrix L . We say the iteration (4) is absolutely stable if

$$h\lambda_i \in S \quad \text{for all } \lambda_i \in \sigma(L). \quad (9)$$

Condition (9) implies that u_n remains bounded for all n . More importantly, (9) is a necessary condition for stable propagation of errors¹. Thus the maximum stable step size is given by

$$H_{\text{stable}} = \max\{h \geq 0 : |R(h\lambda_i)| \leq 1 \text{ for } i = 1, \dots, N\}. \quad (10)$$

As an example, consider the advection equation

$$\frac{\partial}{\partial t}u(x, t) + \frac{\partial}{\partial x}u(x, t) = 0$$

discretized in space by first-order upwind differencing with spatial mesh size Δx

$$U'_i(t) = -\frac{U_i(t) - U_{i-1}(t)}{\Delta x} \quad 0 \leq i \leq N$$

with periodic boundary condition $U_0(t) = U_N(t)$. This is a linear IVP (1) with L a circulant bidiagonal matrix. The eigenvalues of L are plotted in Figure 1(a) for $\Delta x = 1$. Suppose that we wish to integrate this system with the classical fourth-order Runge–Kutta method (2). The time step size must be taken small enough that the scaled spectrum $\{h\lambda_i\}$ lies inside the stability region; Figure 1(c) shows the (maximally) scaled spectrum superimposed on the stability region.

The motivation for this work is that a larger stable step size can be obtained by using a Runge–Kutta method with a larger region of absolute stability. Figure 1(d) shows the stability region of an optimized 10-stage Runge–Kutta method of order four that allows a much larger step size. The ten-stage method was obtained using the technique that is the focus of this work. Since the cost of taking one step is typically proportional to the number of stages s , we can compare the efficiency of methods with different numbers of stages by considering the *effective step size* h/s . Normalizing in this manner, it turns out that the ten-stage method is nearly twice as fast as the traditional four-stage method.

1.3 Design of optimal stability polynomials

We now consider the problem of choosing a stability polynomial so as to maximize the step size under which given stability constraints are satisfied. The resulting nonlinear optimiza-

¹For non-normal L , it may be important to consider the pseudospectrum rather than just the eigenvalues; see Section 3.3.

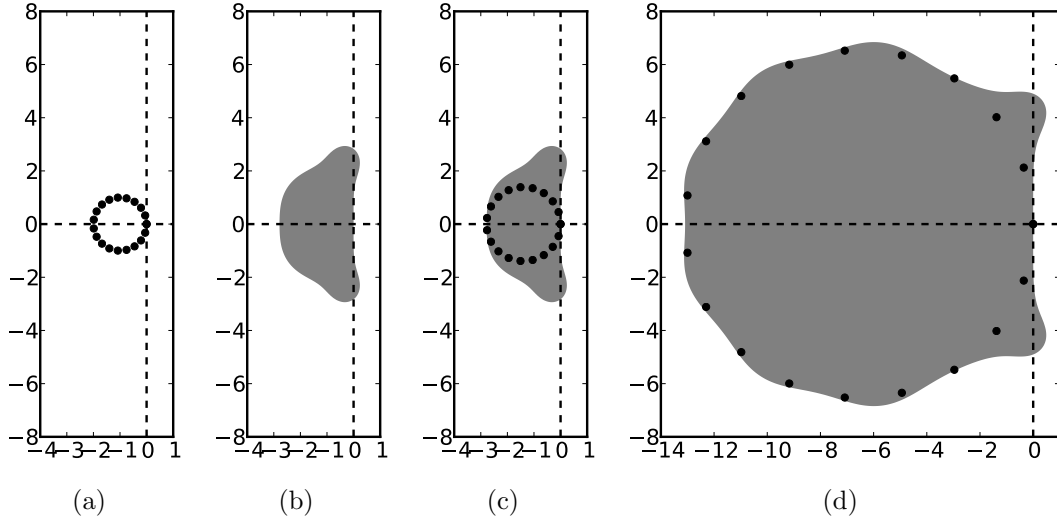


Figure 1: (a) spectrum of first-order upwind difference matrix using $N = 20$ points in space; (b) stability region of the classical fourth-order Runge–Kutta method; (c) Scaled spectrum $h\lambda$ with $h = 1.39$; (d) Scaled spectrum $h\lambda$ for optimal 10-stage method with $h = 6.54$.

tion problem can be written in the general form

$$\begin{aligned} & \underset{x}{\text{maximize}} && f(x) \\ & \text{subject to} && g_i(x) \leq 0 \quad i = 1, \dots, N. \end{aligned}$$

The objective function $f(x)$ is simply the step size h . The stability conditions form N nonlinear inequality constraints:

$$g_i(h, a) = |R(h\lambda_i)| - 1. \tag{11}$$

Here the vector a denotes the coefficients of the stability polynomial (6). Typically one also wishes to impose a minimal order of accuracy. The monomial basis representation (6) of $R(z)$ is then convenient because the first $p + 1$ coefficients $\{a_0, a_1, \dots, a_p\}$ of the stability polynomial are simply taken to satisfy the order conditions (7). As a result, the space of decision variables has dimension $s + 1 - p$, and is comprised of the coefficients $\{a_{p+1}, a_{p+2}, \dots, a_s\}$, as well as the step size h . Then the general optimization problem can be written as

Problem 1 (stability optimization) *Given a spectrum $\{\lambda_i\} \in \mathbb{C}^N$, an order p , and a*

number of stages s , determine h, a in order to

$$\begin{aligned} & \underset{a_{p+1}, a_{p+2}, \dots, a_s, h}{\text{maximize}} && h \\ & \text{subject to} && |R(h\lambda_i)| - 1 \leq 0, \quad i = 1, \dots, N. \end{aligned}$$

We use H_{opt} to denote the solution of Problem 1.

It is sometimes desirable to find a polynomial whose stability region includes not just a finite set of points, but a curve or region Γ in the complex plane. For instance, when L comes from a PDE semi-discretization, it is common for the eigenvalues to fill in some curve as $N \rightarrow \infty$. One might wish to find a method that is stable for any value of N . In Section 3 we approach this by using a set of sample points $\lambda_i \subset \Gamma$; for a discussion of this approach, see [9].

1.4 Previous work

The problem of finding optimal stability regions is of fundamental importance in the numerical solution of initial value problems, and its solution or approximation has been studied by many authors for several decades [24, 33, 39, 17, 18, 19, 42, 22, 21, 31, 23, 32, 40, 28, 27, 1, 3, 2, 41, 6, 36, 35, 5, 4, 26, 29, 37, 34]. Indeed, it is closely related to the problem of finding polynomials of least deviation, which goes back to the work of Chebyshev. A nice review of much of the early work on Runge–Kutta stability regions can be found in [40]. The most-studied cases are those where the eigenvalues lie on the negative real axis, on the imaginary axis, or on a disk in the left half-plane that is tangent to the imaginary axis at the origin. Many results and methods, both exact and numerical, are available for these cases. Much less is available regarding the solution of Problem 1 for arbitrary spectra λ_i .

Two very recent works serve to illustrate both the progress that has been made in solving these problems with nonlinear programming, and the challenges that remain. In [37], optimal schemes are sought for integration of discontinuous Galerkin discretizations of wave equations, where the optimality criteria considered include both accuracy and stability measures. The approach used is based on sequential quadratic programming (local optimization) with many initial guesses. The authors consider methods of at most fourth order and situations with $s - p \leq 4$ “because the cost of the optimization procedure becomes prohibitive for a higher number of free parameters.” In [29], optimally stable polynomials are found for certain spectra of interest for $2 \leq p \leq 4$ and (in a remarkable feat!) s as large as 14. The new methods obtained achieve a 40-50% improvement in efficiency for discontinuous Galerkin integration of the 3D Maxwell equations. The optimization approach employed therein is again a direct search algorithm that does not guarantee a globally optimal solution but “typically converges ... within a few minutes”. However, it was apparently unable to find solutions for $s > 14$ or $p > 4$.

2 An efficient algorithm for design of globally optimal stability polynomials

Finding the global solution of these nonlinear optimization problems in natural form is often quite challenging. Although the Karush-Kuhn-Tucker (KKT) conditions provide necessary conditions for optimality in the solution of nonlinear programming problems, the stability constraints in Problem 1 are nonconvex, hence suboptimal local minima may exist. For problems with convex objective function and convex constraints, the KKT conditions are also sufficient to prove global optimality of a candidate solution, and several methods exist for obtaining optimal solutions in polynomial time. As a result, if an appropriate convex relaxation or decomposition of the general nonlinear problem into convex subexpressions can be found, provably globally optimal solutions (in the case of a relaxation or an approximation, within some error tolerance) can be obtained.

2.1 Reformulation into a sequence of convex problems

The primary theoretical advance leading to the new results in this paper is a reformulation of the problem presented in Section 1.3. Those problem are (for $s > 2$) nonconvex due to the fact that $R(h\lambda_i)$ is a nonconvex function in h (which is one of the decision variables).

Instead of asking for the optimally stable/accurate method we now ask simply whether, for a given step size h , it is possible to construct a stable method:

Problem 2 (feasibility) *Given a spectrum $\{\lambda_i\} \in \mathbb{C}^N$, step size h , order p , and number of stages s ,*

$$\begin{aligned} & \text{find} && a_{p+1}, a_{p+2}, \dots, a_s \\ & \text{subject to} && |R(h\lambda_i)| - 1 \leq 0 \quad i = 1, \dots, N. \end{aligned}$$

Since $R(z)$ depends only linearly on the decision variables a_j , then $|R(z)|$ is convex with respect to a_j . Therefore, Problem 2 is convex. Furthermore, we can reformulate Problem 1 in terms of Problem 2:

Problem 3 *Given a spectrum $\{\lambda_i\} \in \mathbb{C}^N$, order p , and number of stages s ,*

$$\begin{aligned} & \underset{a_{p+1}, a_{p+2}, \dots, a_s}{\text{maximize}} && h \\ & \text{subject to} && \mathbf{Problem\ 2\ feasible.} \end{aligned}$$

Although Problem 3 is not convex, it is an optimization in a single variable. We now introduce a key assumption that allows efficient solution of Problem 3. Although this assumption does not always hold (see below), it leads to an efficient algorithm that works very well in practice.

Assumption 1 *If Problem 2 has a feasible solution for $h = h_0 > 0$, then it has a feasible solution for all $0 \leq h \leq h_0$.*

Assumption 1 is precisely what is required to justify the application of bisection to solve Problem 3. This suggests the following algorithm:

<p>Algorithm 1 (Bisection) <i>Inputs: Positive integers s, p and real numbers ϵ and h_{max} such that $H_{opt} \leq h_{max}$</i> <i>Output: h satisfying $H_{opt} - \epsilon \leq h \leq H_{opt}$</i></p> <pre> h_min = 0 while h_max-h_min>epsilon h = (h_max+h_min)/2 if Problem 3 is feasible h_min = h else h_max = h end end h = h_min </pre>

To see that Assumption 1 does not always hold, take $s = p = 4$; then the stability polynomial (6) is uniquely defined as the degree-four Taylor approximation of the exponential (2), corresponding to the classical fourth-order Runge–Kutta method, which we saw in the introduction. Its stability region is plotted in Figure 1(b). Taking e.g. $\lambda = 0.21 + 2.3i$, one sees that Problem 2 is feasible for $h = 1$ but not for $h = 1/2$.

Although this example shows that Algorithm 1 might formally fail, it concerns only the trivial case $s = p$ in which there is only one possible choice of stability polynomial. We have attempted without success to find a situation with $s > p$ for which Assumption 1 is violated. Algorithm 1 works remarkably well in practice. In all cases we have tested and for which the true H_{opt} is known (see Section 3), Algorithm 1 converges to the globally optimal solution.

The remainder of Section 2 describes in detail the implementation of Algorithm 1.

2.2 Implementation

We have made a prototype implementation of Algorithm 1 in MATLAB. The implementation relies heavily on the CVX package [14, 13], a MATLAB-based modeling system for convex optimization, which in turn relies upon SeDuMi and SDPT3 to provide core interior-point

solver functionality. The convex feasibility problem (Problem 2) can be succinctly stated in four lines of the CVX problem language, and for many cases is solved in under a second by either of the core solvers.

Our implementation re-attempts failed solves (see Section 2.2.2) with the alternate interfaced solver. In our test cases, we observed that the SDPT3 interior-point solver was slower, but more robust than SeDuMi. Consequently, our prototype implementation uses SDPT3 by default.

Using the resulting implementation, we were able to successfully solve problems to within 0.1% accuracy or better with scaled eigenvalue magnitudes $|h\lambda|$ as large as 4000. As an example, comparing with results of [6] for spectra on the real axis with $p = 3, s = 27$, our results are accurate to 6 significant digits.

2.2.1 Least deviation form

The feasibility of Problem 2 can be determined more reliably by reformulating it as a constraint violation minimization problem:

Problem 4 (*Least Deviation*) Given a spectrum $\{\lambda_i\} \in \mathbb{C}^N$, $h \in \mathbb{R}^+$ and $p, s \in \mathbb{N}$

$$\begin{aligned} & \underset{a_{p+1}, a_{p+2}, \dots, a_s}{\text{minimize}} && r \\ & \text{subject to} && r = \max_i (|R(h\lambda_i)| - 1) \quad i = 1, \dots, N. \end{aligned}$$

The objective in Problem 4 is the maximum violation of the constraints from Problem 2. Problem 4 is, in fact, the classical *least deviation* problem, with respect to the set $\{\lambda_i\}$. After solving Problem 4, we can determine the feasibility of the corresponding Problem 2 based on the sign of r . In practice, CVX often returns a small positive objective ($r \approx 10^{-7}$) for values of h that are just feasible. Hence the bisection step is accepted if $r < \epsilon$ where $\epsilon \ll 1$. The results are generally insensitive (up to the first few digits) to the choice of ϵ over a large range of values; we have used $\epsilon = 10^{-7}$ for all results in this work. Bisection based on Problem 4 typically leads to more accurate solutions than that based on Problem 2 for both SeDuMi and SDPT3, but the accuracy that can be achieved is eventually limited by the need to choose a suitable value ϵ .

2.2.2 Conditioning and change of basis

Unfortunately, for large values of $h\lambda_i$, the numerical solution of Problem 2 becomes difficult due to ill-conditioning of the constraint matrix. Observe from (6) that the constrained quantities $R(h\lambda_i)$ are related to the decision variables a_j through multiplication by a Vandermonde matrix. Vandermonde matrices are known to be ill-conditioned for most choices of

abscissas. For very large $h\lambda_i$, the resulting CVX problem cannot be reliably solved by either of the core solvers.

A first approach to reducing the condition number of the constraint matrix is to rescale the monomial basis. We have found that a more robust approach for many types of spectra can be obtained by choosing a basis that is approximately orthogonal over the given spectrum $\{\lambda_i\}$. Thus we seek a solution of the form

$$R(z) = \sum_{j=0}^s a_j q_j(z) \quad \text{where} \quad q_j(z) = \sum_{k=0}^j b_{jk} z^k. \quad (12)$$

Here $q_j(z)$ is a degree- j polynomial chosen to give a well-conditioned constraint matrix, and b_{jk} are the corresponding coefficients. The choice of the basis $q_j(z)$ is a challenging problem in general. In the special case when the spectrum is real and negative, an obvious choice is the basis of Chebyshev polynomials, shifted and scaled to the domain $[hx, 0]$ where $x = \min_i \operatorname{Re}(\lambda_i)$, via an affine map:

$$q_j(z) = T_j \left(1 + \frac{2z}{hx} \right), \quad (13)$$

where T_j is the degree- j Chebyshev polynomial of the first kind. The motivation for using this basis is that when the eigenvalues λ_i lie on the negative real axis, then we have $|q_j(h\lambda_i)| \leq 1$ for all i . This basis is also suggested by the fact that $q_j(z)$ is the optimal stability polynomial in terms of negative real axis inclusion for $p = 1, s = j$. In Section 3, we will see that this choice of basis works well for more general spectra when the largest magnitude eigenvalues lie near the negative real axis.

The drawback of not using the monomial basis is that the dimension of the problem is $s + 1$ (rather than $s + 1 - p$) and we must now impose the order conditions explicitly:

$$\sum_{j=0}^s a_j b_{jk} = \frac{1}{k!} \quad \text{for } k = 0, 1, \dots, p. \quad (14)$$

Consequently, using a non-monomial basis increases the number of design variables in the problem and introduces a tiny, but usually very poorly conditioned equality constraint matrix $B \in \mathbb{R}^{p \times s}$. However, it can dramatically improve the conditioning of the inequality constraints.

As an example, we consider a spectrum of 3200 equally spaced values λ_i in the interval $[-1, 0]$. The exact solution is known to be $h = 2s^2$. Figure 2 shows the relative error as well as the inequality constraint matrix condition number obtained by using the monomial (6) and Chebyshev (13) bases. Typically, the solver is accurate until the condition number

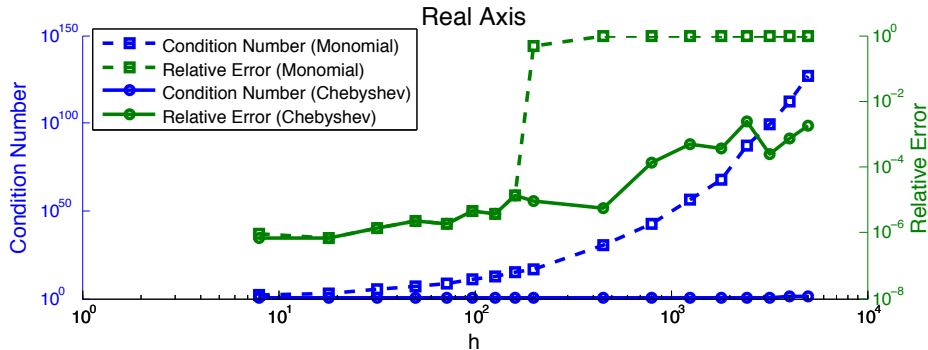


Figure 2: Condition number of principal constraint matrix and relative solution accuracy versus optimal step size.

reaches about 10^{16} . This supports the hypothesis that it is the conditioning of the inequality constraint matrix that leads to failure of the solver. The Chebyshev basis keeps the condition number small and yields accurate answers even for very large values of h .

3 Optimal stability polynomials

We now demonstrate the effectiveness of our algorithm by applying it to determine optimally stable polynomials (i.e., solve Problem 1) for various types of spectra.

3.1 Verification

In this section we apply our algorithm to some well-studied cases with known exact or approximate results, in order to verify its accuracy and correctness. In addition to the real axis, imaginary axis, and disk cases below, we have successfully recovered the results of [29]. Our algorithm succeeds in finding the globally optimal solution in every case for which it is known, except in some cases of extremely large step sizes for which the underlying solvers (SDPT3 and SeDuMi) eventually fail. The successful global solution of such a variety of test cases provides strong empirical justification for the use of bisection.

3.1.1 Negative real axis inclusion

Here we consider the largest h such that $[-h, 0] \in S$. This is the most heavily studied case in the literature, as it applies to the semi-discretization of parabolic PDEs and a large increase of H_{opt} is possible when s is increased (see, e.g., [33, 40, 28, 6, 34]). For first order accurate

Stages	H_{opt}/s^2				
	$p = 1$	$p = 2$	$p = 3$	$p = 4$	$p = 10$
1	2.000				
2	2.000	0.500			
3	2.000	0.696	0.279		
4	2.000	0.753	0.377	0.174	
5	2.000	0.778	0.421	0.242	
6	2.000	0.792	0.446	0.277	
7	2.000	0.800	0.460	0.298	
8	2.000	0.805	0.470	0.311	
9	2.000	0.809	0.476	0.321	
10	2.000	0.811	0.481	0.327	0.051
15	2.000	0.817	0.492	0.343	0.089
20	2.000	0.819	0.496	0.349	0.120
25	2.000	0.820	0.498	0.352	0.125
30	2.001	0.821	0.499	0.353	0.129
35	2.000	0.821	0.499	0.354	0.132
40	2.000	0.821	0.500	0.355	0.132

Table 1: Scaled size of real axis interval inclusion for optimized methods.

methods ($p = 1$), the optimal polynomials are just shifted Chebyshev polynomials, and the optimal timestep is $H_{\text{opt}} = 2s^2$. Many special analytical and numerical techniques have been developed for this case; the most powerful seems to be that of Bogatyrev [6].

We apply our algorithm, taking $N = 6400$ evenly-spaced values $\lambda_i \in [-1, 0]$ and using the shifted and scaled Chebyshev basis (13). Results for up to $s = 40$ are shown in Table 1 (note that we list H_{opt}/s^2 for easy comparison, since H_{opt} is approximately proportional to s^2 in this case). We include results for $p = 10$ to demonstrate the algorithm's ability to handle high-order methods. For $p = 1, 2$, the values computed here match those available in the literature [39]. Most of the values for $p = 3, 4$ and 10 are new results. Figure 3 shows some examples of stability regions for optimal methods. As observed in the literature, it seems that H_{opt}/s^2 tends to a constant (that depends only on p) as s increases.

3.1.2 Imaginary axis inclusion

Next we consider the largest h such that $[-ih, ih] \in S$. Optimal polynomials for imaginary axis inclusion have also been studied by many authors, and a number of exact results are known or conjectured [39, 42, 21, 22, 23, 40]. We again approximate the problem, taking $N = 3200$ evenly-spaced values in the interval $[0, i]$ (note that stability regions are necessarily

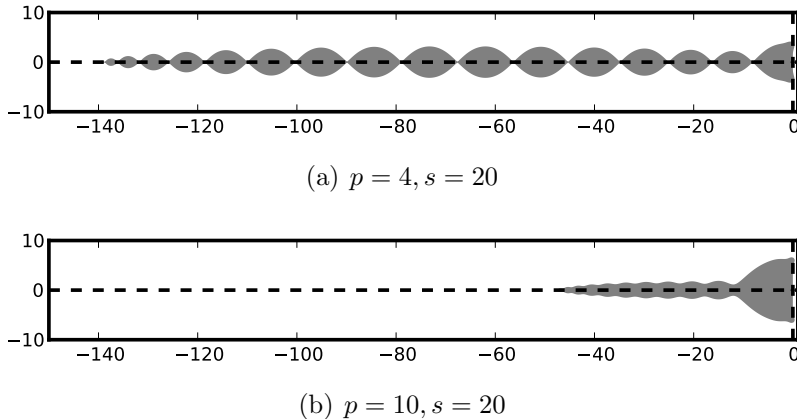


Figure 3: Stability regions of some optimal methods for real axis inclusion.

symmetric about the real axis since $R(z)$ has real coefficients). We use a “rotated” Chebyshev basis defined by

$$q_j(z) = i^j T_j \left(\frac{iz}{hx} \right),$$

where $x = \max_i(|\operatorname{Im}(\lambda_i)|)$. Like the Chebyshev basis for the negative real axis, this basis dramatically improves the robustness of the algorithm for imaginary spectra. Table 2 shows the optimal effective step sizes. In agreement with [39, 22], we find $H = s - 1$ for $p = 1$ (all s) and for $p = 2$ (s odd). We also find $H = s - 1$ for $p = 1$ and s even, which was conjectured in [42] and confirmed in [40]. We find $H_{\text{opt}} = \sqrt{s(s-2)}$ for $p = 2$ and s even, strongly suggesting that the polynomials given in [21] are optimal for these cases; on the other hand, our results show that those polynomials, while third order accurate, are not optimal for $p = 3$ and s odd. Figure 4 shows some examples of stability regions for optimal methods.

3.1.3 Disk inclusion

Additional attention has been paid to stability regions that include the disk

$$D(h) = \{z : |1 + z/h| \leq 1\}, \quad (15)$$

for the largest possible h . The optimal result for $p = 1$ ($H_{\text{opt}} = s$) was first proved by Jeltsch & Nevanlinna [17]. The optimal result for $p = 2$ ($H_{\text{opt}} = s - 1$) was first proved in [42]. Both results have been unwittingly rediscovered by later authors. For $p > 2$, no exact results are available.

Stages	H_{opt}/s			
	$p = 1$	$p = 2$	$p = 3$	$p = 4$
2	0.500			
3	0.667	0.667	0.577	
4	0.750	0.708	0.708	0.707
5	0.800	0.800	0.783	0.693
6	0.833	0.817	0.815	0.816
7	0.857	0.857	0.849	0.813
8	0.875	0.866	0.866	0.866
9	0.889	0.889	0.884	0.864
10	0.900	0.895	0.895	0.894
15	0.933	0.933	0.932	0.925
20	0.950	0.949	0.949	0.949
25	0.960	0.960	0.959	0.957
30	0.967	0.966	0.966	0.966
35	0.971	0.971	0.971	0.970
40	0.975	0.975	0.975	0.975
45	0.978	0.978	0.978	0.977
50	0.980	0.980	0.980	0.980

Table 2: Scaled size of imaginary axis inclusion for optimized methods.

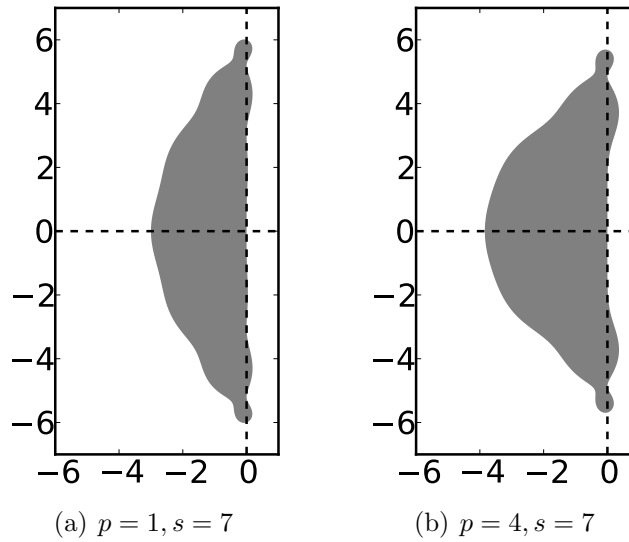


Figure 4: Stability regions of some optimal methods for imaginary axis inclusion.

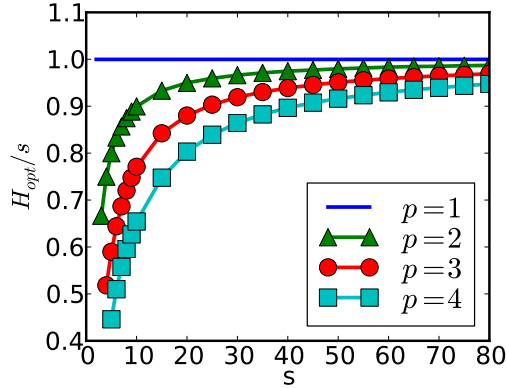


Figure 5: Relative size of largest disk that can be included in the stability region (scaled by the number of stages).

We use the basis

$$q_j(z) = \left(1 + \frac{z}{h}\right)^j.$$

The basis polynomial $q_j(z)$ is actually the optimal solution for the case $s = j$, $p = 1$. This basis can also be motivated by recalling that Vandermonde matrices are perfectly conditioned when the points involved are equally spaced on the unit circle. Our basis can be obtained by taking the monomial basis and applying an affine transformation that shifts the unit circle to the disk (15). This basis greatly improves the robustness of the algorithm for this particular spectrum. We show results for $p \leq 4$ in Figure 5. For $p = 3$ and $s = 5, 6$, our results give a small improvement over those of [20]. Some examples of optimal stability regions are plotted in Figure 6.

3.2 Spectrum with a gap

We now demonstrate the effectiveness of our method for more general spectra. First we consider the case of a dissipative problem with two time scales, one much faster than the other. This type of problem was the motivation for the development of projective integrators [11]. Following the ideas outlined there we consider the union of the following regions:

$$D_1(h) = \{z : |z| \leq 1, \Re(z) \leq 0\} \tag{16a}$$

$$D_2(h) = \{z : |z - \alpha| \leq 1\}. \tag{16b}$$

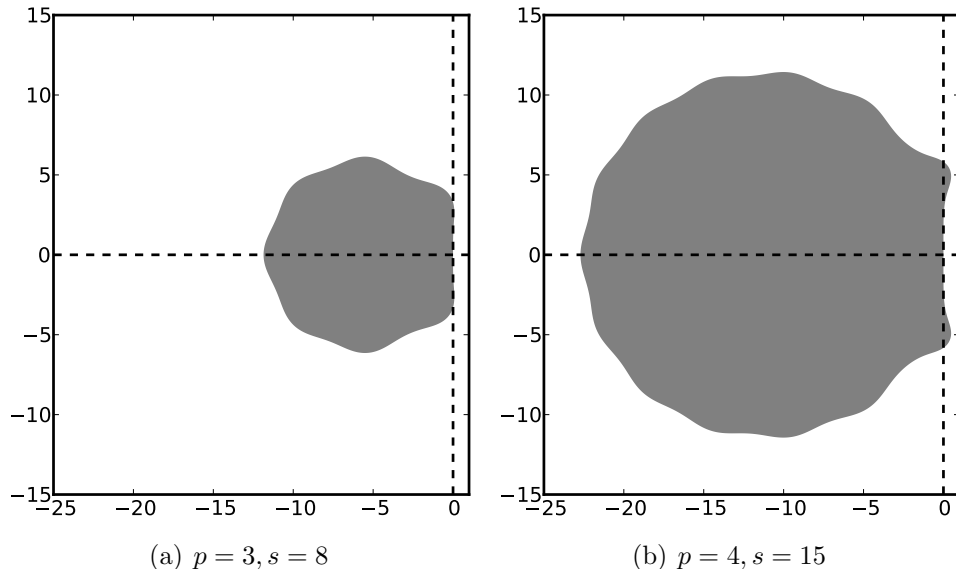


Figure 6: Stability regions of some optimal methods for disk inclusion.

We take $\alpha = 20$ and use the shifted and scaled Chebyshev basis (13). Results are shown in Figure 7. A dramatic increase in efficiency is achieved by adding a few extra stages.

3.3 Legendre pseudospectral discretization

Next we consider a system obtained from semidiscretization of the advection equation on the interval $[-1, 1]$ with homogeneous Dirichlet boundary condition:

$$u_t = u_x \quad u(t, x = 1) = 0.$$

The semi-discretization is based on pseudospectral collocation at points given by the zeros of the Legendre polynomials; we take $N = 50$ points. The semi-discrete system takes the form (1), where L is the Legendre differentiation matrix, whose eigenvalues are shown in Figure 8(a). We compute an optimally stable polynomial based on the spectrum of the matrix, taking $s = 7$ and $p = 1$. The stability region of the resulting method is plotted in Figure 8(c). Using an appropriate step size, all the scaled eigenvalues of L lie in the stability region. Yet this method is unstable in practice for any positive step size; Figure 8(e) shows an example of a computed solution after three steps, where the initial condition is a Gaussian. The resulting instability is non-modal, meaning that it does not correspond to any of the eigenvectors of L (compare [10, Figure 31.2]).

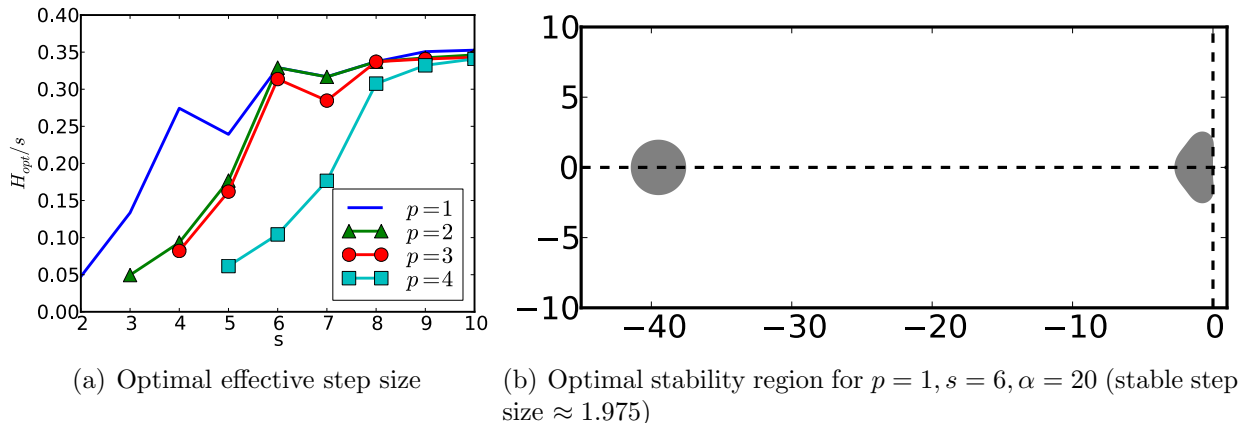


Figure 7: Optimal methods for spectrum with a gap (16) with $\alpha = 20$.

This discretization is now well-known as an example of non-normality [10, Chapters 30–32]. Due to the non-normality, it is necessary to consider the pseudospectrum in order to design an appropriate integration scheme. The pseudospectrum and eigenvalues are shown in Figure 8(b); the instability occurs because the stability region does not contain an interval on the imaginary axis about the origin, whereas the pseudospectrum includes such an interval.

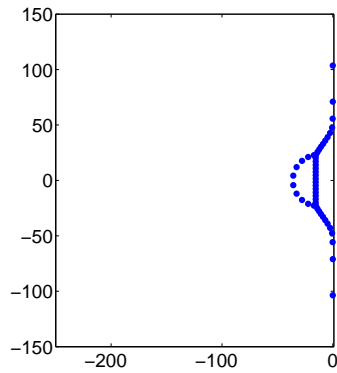
Next we instead compute an optimally stable integrator based on the ϵ -pseudospectrum (see [10]), which is the set

$$\{z \in \mathbb{C} : \|(z - D)^{-1}\| > 1/\epsilon\}.$$

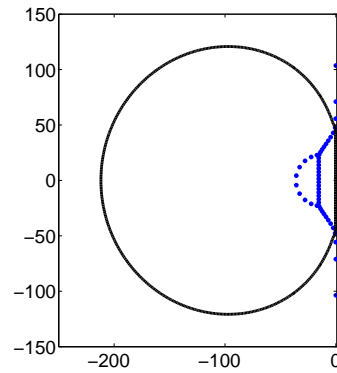
We take $\epsilon = 2$. The pseudospectrum is computed using an approach proposed in [38, Section 20], with sampling on a fine grid. In order to reduce the number of constraints and speed up the solution, we compute the convex hull of the resulting set and apply our algorithm. The resulting stability region is shown in Figure 8(d). It is remarkably well adapted; notice the two isolated roots that ensure stability of the modes corresponding to the extremal imaginary eigenvalues. We have verified that this method produces a stable solution, in agreement with theory [10]; Figure 8(f) shows an example of a solution computed with this method. The initial Gaussian pulse advects to the left.

3.4 Thin rectangles

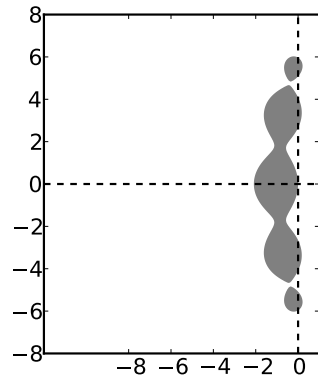
A major application of explicit Runge–Kutta methods with many stages is the solution of moderately stiff advection–reaction–diffusion problems [16, 41]. For such problems, the stability region must include a large interval on the negative real axis, but also some region around it (due to convection term(s)). If centered differences are used for the advective



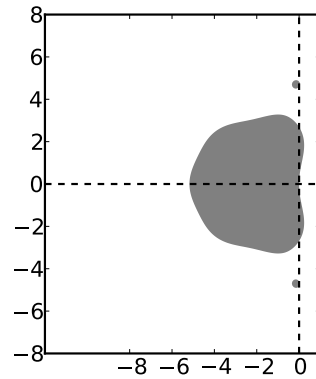
(a) Eigenvalues.



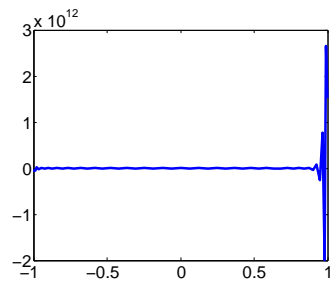
(b) Eigenvalues and pseudospectrum (the boundary of the 2-pseudospectrum is plotted).



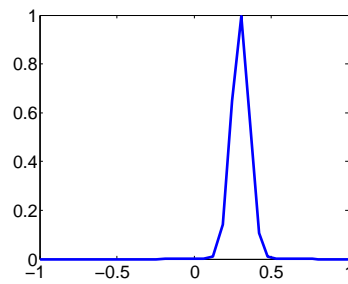
(c) Optimized stability region based on eigenvalues.



(d) Optimized stability region based on pseudospectrum.



(e) Solution computed with method based on spectrum.



(f) Solution computed with method based on pseudospectrum.

Figure 8: Results for the Legendre differentiation matrix with $N = 50$.

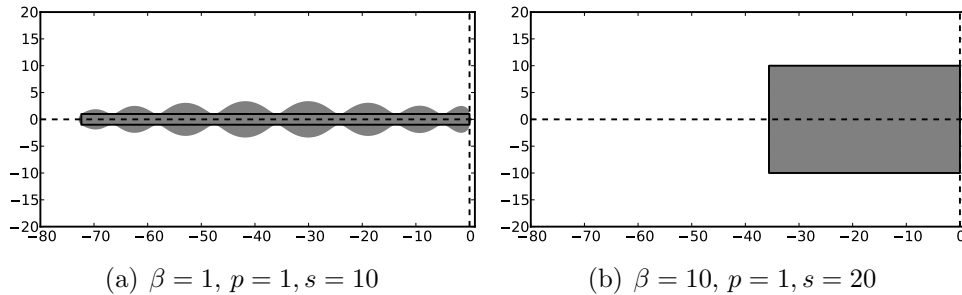


Figure 9: Stability regions of some optimal methods for thin rectangle inclusion.

terms, it is natural to require that a small interval on the imaginary axis be included. Hence one may be interested in methods that contain the rectangular region

$$\Gamma_\kappa = \{\lambda \in \mathbb{C} : -\beta \leq \text{Im}(\lambda) \leq \beta, \quad -\kappa \leq \text{Re}(\lambda) \leq 0\}. \quad (17)$$

for given κ, β . No methods optimized for such regions appear in the literature, and the available approaches for devising methods with extended real axis stability (including those of [36]) cannot be applied to such regions. Because of this, previously existing methods are applicable only if upwind differencing is applied to convective terms [41, 36].

For this example, rather than parameterizing by the step size h , we assume a desired step size h and imaginary axis limit β are given based on the convective terms (which generally require small step sizes for accurate resolution). We seek to find (for given s, p) the polynomial (6) that includes Γ_κ for κ as large as possible. This could correspond to selection of an optimal integrator based on the ration of convective and diffusive scales (roughly speaking, the Reynolds number). Since the desired stability region lies relatively near the negative real axis, we use the shifted and scaled Chebyshev basis (13).

Stability regions of some optimal methods are shown in Figure 9. The outline of the included rectangle is superimposed in black. The stability region for $\beta = 10, s = 20$, shown in Figure 9 is especially interesting as it is almost exactly rectangular!

An interesting theoretical question arises in this context. As we have seen, roughly speaking, for negative real axis inclusion $H_{\text{opt}} \propto Cs^2$ for some constant C but for inclusion of the imaginary axis or a disk, $H_{\text{opt}} \propto Cs$. One may ask in general, which class of spectra leads to each of these (or other) types of behavior. The question can be formulated more precisely as follows:

Given a family of regions $\Gamma_\kappa \in \mathbb{C}$ (parameterized by κ) such that $\max_{\alpha \in \Gamma_\kappa} |\alpha| = \mathcal{O}(\kappa)$, let H_{opt} be the maximum value of h such that there exists a polynomial (6) of degree s whose stability region includes $h\Gamma_\kappa$. How does H_{opt} vary with s as $s \rightarrow \infty$?

Experimental results indicate that for Γ_κ corresponding to a long thin rectangle of fixed width, we do indeed have $H_{\text{opt}} \propto s^2$. Based on experiments so far, it seems likely that H_{opt} grows quadratically with s as long as the maximum absolute real part of Γ_κ is fixed, but not if the maximum absolute real part grows linearly with κ . Our algorithm can be used to explore this and similar questions.

References

- [1] A. ABDULLE, *On roots and error constants of optimal stability polynomials*, BIT Numerical Mathematics, 40 (2000), pp. 177–182.
- [2] ———, *Fourth order Chebyshev methods with recurrence relation*, SIAM Journal on Scientific Computing, 23 (2002), pp. 2041–2054.
- [3] A. ABDULLE AND A. MEDOVIKOV, *Second order Chebyshev methods based on orthogonal polynomials*, Numerische Mathematik, 90 (2001), pp. 1–18.
- [4] V. ALLAMPALLI, R. HIXON, M. NALLASAMY, AND S. D. SAWYER, *High-accuracy large-step explicit RungeKutta (HALE-RK) schemes for computational aeroacoustics*, Journal of Computational Physics, 228 (2009), pp. 3837–3850.
- [5] M. BERNARDINI AND S. PIROZZOLI, *A general strategy for the optimization of Runge-Kutta schemes for wave propagation phenomena*, Journal of Computational Physics, 228 (2009), pp. 4182–4199.
- [6] A. B. BOGATYREV, *Effective solution of the problem of the optimal stability polynomial*, Sbornik: Mathematics, 196 (2005), pp. 959–981.
- [7] J. BUTCHER, *Numerical Methods for Ordinary Differential Equations*, Wiley, second ed., 2008.
- [8] T. DAVIDSON, *Enriching the Art of FIR Filter Design via Convex Optimization*, IEEE Signal Processing Magazine, 27 (2010), pp. 89–101.
- [9] S. ELLACOTT, *Linear Chebyshev approximation in the complex plane using Lawson’s algorithm*, Mathematics of Computation, (1976).
- [10] M. EMBREE AND L. TREFETHEN, *Spectra and Pseudospectra: The Behavior of Non-normal Matrices and Operators*, Princeton University Press, Princeton, 2005.

- [11] C. W. GEAR AND I. G. KEVREKIDIS, *Projective Methods for Stiff Differential Equations: Problems with Gaps in Their Eigenvalue Spectrum*, SIAM Journal on Scientific Computing, 24 (2003), p. 1091.
- [12] S. GOTTLIEB, D. I. KETCHESON, AND C.-W. SHU, *Strong Stability Preserving Runge–Kutta and Multistep Time Discretizations*, World Scientific Publishing Company, 2011.
- [13] M. GRANT AND S. BOYD, *Graph implementations for nonsmooth convex programs*, in Recent Advances in Learning and Control, V. Blondel, S. Boyd, and H. Kimura, eds., Lecture Notes in Control and Information Sciences, Springer-Verlag Limited, 2008, pp. 95–110.
- [14] ———, *CVX: MATLAB software for disciplined convex programming*. <http://cvxr.com/cvx>, Apr. 2011.
- [15] E. HAIRER, , AND G. WANNER, *Solving ordinary differential equations II: Stiff and differential-algebraic problems*, Springer, second ed., 1996.
- [16] W. HUNSDORFER AND J. G. VERWER, *Numerical solution of time-dependent advection-diffusion-reaction equations*, vol. 33, Springer, 2003.
- [17] R. JELTSCH AND O. NEVANLINNA, *Largest disk of stability of explicit Runge–Kutta methods*, BIT Numerical Mathematics, 18 (1978), pp. 500–502.
- [18] ———, *Stability of explicit time discretizations for solving initial value problems*, Numerische Mathematik, 37 (1981), pp. 61–91.
- [19] ———, *Stability and accuracy of time discretizations for initial value problems*, Numerische Mathematik, 40 (1982), pp. 245–296.
- [20] R. JELTSCH AND M. TORRILHON, *Flexible Stability Domains for Explicit Runge–Kutta Methods*, Some topics in industrial and applied mathematics, (2007), p. 152.
- [21] I. P. KINNMARK AND W. G. GRAY, *One step integration methods of third-fourth order accuracy with large hyperbolic stability limits*, Mathematics and Computers in Simulation, 26 (1984), pp. 181–188.
- [22] ———, *One step integration methods with maximum stability regions*, Mathematics and Computers in Simulation, 26 (1984), pp. 87–92.
- [23] I. P. E. KINNMARK AND W. G. GRAY, *Fourth-order accurate one-step integration methods with large imaginary stability limits*, Numerical Methods for Partial Differential Equations, 2 (1986), pp. 63–70.

- [24] J. LAWSON, *An order five Runge–Kutta process with extended region of stability*, SIAM Journal on Numerical Analysis, (1966).
- [25] R. J. LEVEQUE, *Finite Difference Methods for Ordinary and Partial Differential Equations*, SIAM, Philadelphia, 2007.
- [26] J. MARTIN-VAQUERO AND B. JANSSEN, *Second-order stabilized explicit Runge–Kutta methods for stiff problems*, Computer Physics Communications, 180 (2009), pp. 1802–1810.
- [27] J. L. MEAD AND R. A. RENAUT, *Optimal Runge–Kutta methods for first order pseudospectral operators*, Journal of Computational Physics, 152 (1999), pp. 404–419.
- [28] A. A. MEDOVIKOV, *High order explicit methods for parabolic equations*, BIT Numerical Mathematics, 38 (1998), pp. 372–390.
- [29] J. NIEGEMANN, R. DIEHL, AND K. BUSCH, *Efficient low-storage RungeKutta schemes with optimized stability regions*, Journal of Computational Physics, 231 (2011), pp. 372–364.
- [30] M. PARSANI ET AL., *Optimal explicit runge–kutta schemes for the spectral difference method applied to euler and linearized euler equations*. in preparation.
- [31] J. PIKE AND P. ROE, *Accelerated convergence of Jameson’s finite-volume Euler scheme using van der Houwen integrators*, Computers & Fluids, 13 (1985), pp. 223–236.
- [32] R. A. RENAUT, *Two-step Runge–Kutta methods and hyperbolic partial differential equations*, mathematics of computation, (1990).
- [33] W. RIHA, *Optimal stability polynomials*, Computing, 9 (1972), pp. 37–43.
- [34] L. M. SKVORTSOV, *Explicit stabilized Runge–Kutta methods*, Computational Mathematics and Mathematical Physics, 51 (2011), pp. 1153–1166.
- [35] B. SOMMEIJER AND J. G. VERWER, *On stabilized integration for time-dependent PDEs*, Journal of Computational Physics, 224 (2007), pp. 3–16.
- [36] M. TORRILHON AND R. JELTSCH, *Essentially optimal explicit RungeKutta methods with application to hyperbolicparabolic equations*, Numerische Mathematik, 106 (2007), pp. 303–334.

- [37] T. TOULORGE AND W. DESMET, *Optimal Runge–Kutta Schemes for Discontinuous Galerkin Space Discretizations Applied to Wave Propagation Problems*, Journal of Computational Physics, (2011).
- [38] L. TREFETHEN, *Computation of pseudospectra*, Acta numerica, (1999).
- [39] P. VAN DER HOUWEN, *Explicit Runge–Kutta Formulas with Increased Stability Boundaries*, Numerische Mathematik, 20 (1972), pp. 149–164.
- [40] P. J. VAN DER HOUWEN, *The development of Runge–Kutta methods for partial differential equations*, Applied numerical mathematics, (1996).
- [41] J. G. VERWER, B. SOMMEIJER, AND W. HUNSDORFER, *RKC time-stepping for advection-diffusion-reaction problems*, Journal of Computational Physics, 201 (2004), pp. 61–79.
- [42] R. VICHNEVETSKY, *New stability theorems concerning one-step numerical methods for ordinary differential equations*, Mathematics and Computers in Simulation, 25 (1983), pp. 199–205.